RESEARCH ARTICLE

Leigh A. Mrotek · Martha Flanders · John F. Soechting

Oculomotor responses to gradual changes in target direction

Abstract Smooth pursuit tracking of targets moving linearly (in one dimension) is well characterized by a model where retinal image motion drives eye acceleration. However, previous findings suggest that this model cannot be simply extended to two-dimensional (2D) tracking. To examine 2D pursuit, in the present study, human subjects tracked a target that moved linearly and then followed the arc of a circle. The subjects' gaze angular velocity accurately matched target angular velocity, but the direction of smooth pursuit always lagged behind the current target direction. Pursuit speed slowly declined after the onset of the curve (for about 500 ms), even though the target speed was constant. In a second experiment, brief perturbations were presented immediately prior to the beginning of the change in direction. The subjects' responses to these perturbations consisted of two components: (1) a response specific to the parameters of the perturbation and (2) a nonspecific response that always consisted of a transient decrease in gaze velocity. With the exception of this nonspecific response, pursuit behavior in response to the gradual changes in direction and to the perturbations could be explained by using retinal slip (image velocity) as the input signal. The retinal slip was parallel and perpendicular to the instantaneous direction of pursuit ultimately resulted in changes in gaze velocity (via gaze acceleration). Perhaps due to the subjects' expectations that the target will curve, the sensitivity to the image motion in the direction of pursuit was not as strong as the sensitivity to image motion perpendicular to gaze velocity.

Keywords Smooth pursuit · Direction · Speed · Retinal slip

L. A. Mrotek · M. Flanders · J. F. Soechting (✉)
Department of Neuroscience, University of Minnesota,
6-145 Jackson Hall, 321 Church Street SE, Minneapolis,
MN 55455, USA
E-mail: soech001@umn.edu
Tel.: +1-612-6257961
Fax: +1-612-6265009

Introduction

For targets moving in one dimension, smooth pursuit tracking has been extensively studied (reviewed by Keller and Heinen 1991; Krauzlis 2004; Lisberger et al. 1987), and the error signals (image motion) that drive this behavior are well understood (Krauzlis and Lisberger 1989, 1994a; Robinson et al. 1986). Feedback models in which eye acceleration is proportional to retinal image velocity and acceleration generate predictions that provide a good match to experimental data. However, an additional component (a motion transient), which is not scaled with the parameters of target or image motion, is needed to account for smooth pursuit behavior at the onset of tracking (Krauzlis and Lisberger 1994a).

It is also recognized that feedback models do not provide a complete description of the behavior in all conditions (Collewijn and Tamminga 1984; Fender 1971; Kowler and Steinman 1981; Kowler et al. 1984). For example, a target that moves predictably (such as sinusoidally) can be tracked with a time delay close to zero (Kettner et al. 1996). If a target always begins moving in the same direction, or if it consistently changes direction at a specified location, the target motion in previous trials influences the smooth pursuit behavior in the current trial (Kowler 1989). Direct cognitive expectations play an even stronger role. For instance, when given a verbal or visual cue, the eyes move in the cued direction instead of the direction predicted by the previous trials (Kowler 1989).

Tracking of targets that move along two-dimensional trajectories has been less well studied. However, it is clear that feedback models in which there is independent control of smooth pursuit along two orthogonal directions cannot fully account for the experimental observations. For example, a perturbation along one direction affects smooth pursuit in the perpendicular direction (Leung and Kettner 1997) and tracking errors are smallest when the target speed follows the "two-thirds

power'' relating speed and curvature (de'Sperati and Viviani 1997). Furthermore, the gain of smooth pursuit exhibits directional anisotropies that depend on the tracking conditions (Schwartz and Lisberger 1994).

In our laboratory, when subjects tracked a target that moved in a straight line and abruptly changed direction, the latencies for the changes in speed and direction of pursuit differed (Engel et al. 1999, 2000). A subsequent more detailed analysis (Soechting et al. 2005) showed that the pursuit following an abrupt change in target direction could be represented as the vector summation of two responses: (1) to the cessation of target motion in the original direction, and (2) to the onset of target motion in the new direction. The two responses had different latencies and the gain of the second showed directional dependencies.

Visual targets do not usually change direction abruptly, except in games, such as pool and tennis. Furthermore, it seemed unlikely that this two-component model that could account for the response to an abrupt change in target direction could also account for the pursuit of targets that changed direction smoothly and continuously because it would imply intermittent control of smooth pursuit (but see Roitman et al. 2004). Therefore, in the present experiments we investigated the smooth pursuit response to targets that followed a circular arc. The radius of curvature and length of the arc varied unpredictably from trial to trial. In another experiment, we measured the directional gain of smooth pursuit by applying brief perturbations. Image motion feedback models of the type described earlier were able to account for most aspects of the behavior. However, the results suggest directional anisotropies in the gain of smooth pursuit in this condition, and these anisotropies depend on the instantaneous direction of pursuit.

Methods

Subjects

Nine subjects participated in a total of 20 experimental sessions. The procedures were approved by the University of Minnesota Institutional Review Board and all subjects gave their informed consent, had normal or corrected to normal vision, and had no history of neurological disorders.

Stimulus presentation and data recording

Subjects visually tracked a target presented on a computer monitor. They sat unrestrained in a chair with a rigid back support and with the eyes 85 cm from the screen. The room lighting was dimmed and the seat height was adjusted so that the screen was viewed comfortably. Each trial began with a cue target (size = 0.15° of visual angle, °va) at a position that the tracking target would cross approximately 100 ms after it started moving.

The trial was initiated when the subject fixated the cue target. The round tracking target (size = 0.1°va) always began moving horizontally (x-direction) from left to right. When the target approached the center of the screen, in most trials (89%) it began to change direction by traveling along the perimeter of a circle. In 11% of the trials the target continued to travel straight across the screen. The time at which direction began to change was randomized with a uniform distribution within a 1 s interval. On average, the target changed direction at the center of the screen. The magnitude of the direction change, the radius of curvature and the target angular velocity also varied randomly from trial to trial. Each experiment typically required two to four sessions and subjects could take breaks ad libitum.

Eye movements were measured with a head-mounted infrared camera system (SMI Eye Link System). Two cameras recorded the position of the pupils relative to the head, and another camera recorded the position of the head relative to the computer monitor. This set-up allowed us to calculate the position at which gaze intersected the screen. The sampling rate of the cameras was 250 Hz. The system was calibrated prior to data collection and at any time the head mounted camera position was changed; a drift correction was performed prior to every trial. In previous experiments head movement was shown to be minimal (Engel and Soechting 2003), with average correlation coefficients between gaze velocity and eye-in-head velocity exceeding 0.96 (for direction of motion $r = 0.977$, and for speed $r = 0.964$).

Under our experimental conditions, the spatial resolution (SD during fixation) was 0.06 ± 0.04°va, and the accuracy (mean error over a range of targets spanning the display) averaged 0.4 ± 0.2°va. During fixation, the RMS of gaze velocity averaged 2.3°va/s.

Tracking curvilinear motion (Experiment 1)

Five subjects, two females and three males (21–49 years), volunteered for the first experiment, tracking a target that initially moved in a straight line and then followed a circular path at a constant speed. Direction was defined in degrees of polar angle (°pa), with downward defined as 0°pa, and counterclockwise motion resulting in a positive change in direction. The target's speed (S_T; °va/s) was defined by its radius of curvature (R; °va) and the angular velocity $(\dot{\Theta}_T;\ \deg \mathrm{pa/s})$:

$$S_T = R \times \dot{\Theta}_T. \tag{1}$$

Direction changed by amounts that ranged from −240 to 240°pa in 60°pa increments (Fig. 1a). The radius of curvature could take on one of five values, ranging from 1.08 to 3.96°va (1.62–5.94 cm). At all but the largest radius, the angular velocities could have one of three values, ranging from 100 to 400°pa/s (see Table 1). The resulting range of target speeds was
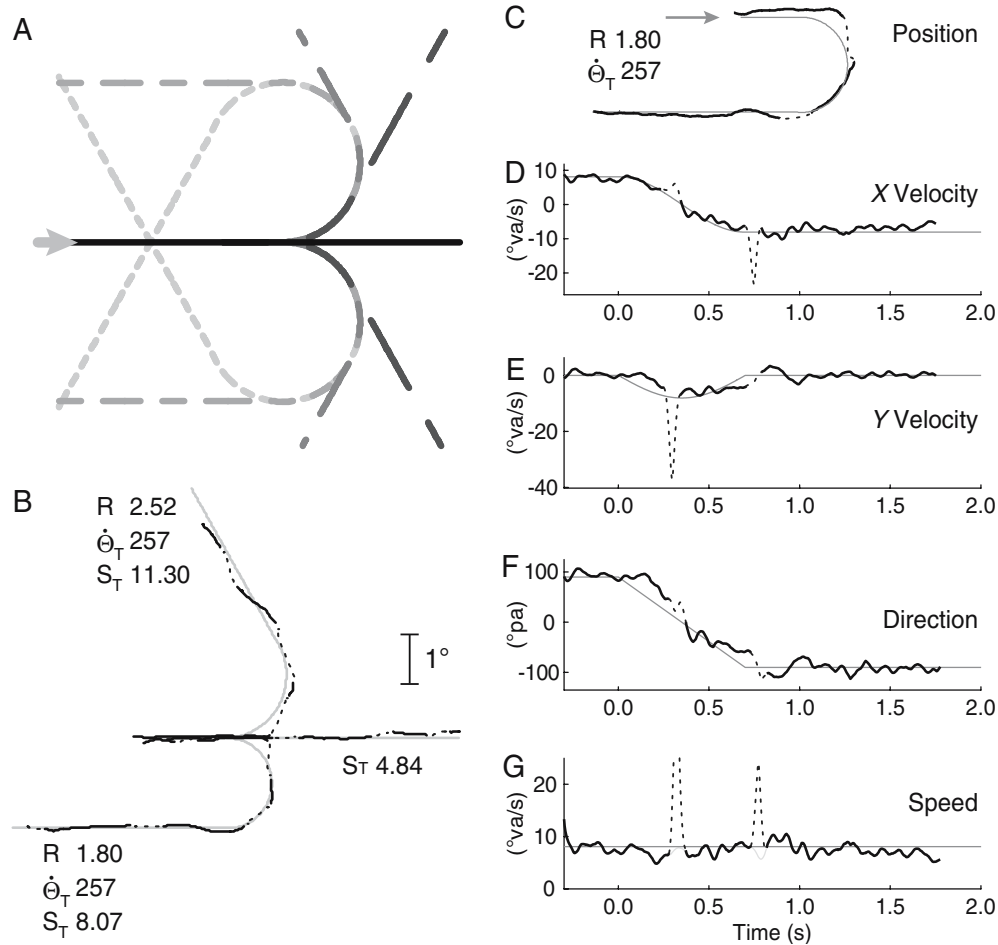
Fig. 1 a Schematic of target paths for all possible magnitudes of direction change (*angles*) for one radius of curvature. The beginning of the target path is removed, but all targets started at the farthest left center portion of the screen and traveled to the right towards the center of the screen (*gray arrow*). The target followed a circular path for $\pm60°$pa (*dark gray, long dashes*) to $\pm240°$pa (*light gray, short dashes*) in $60°$ increments in the counterclockwise (*positive*) or clockwise direction (*negative*). **b** Three representative trials from one subject are shown. The *thin gray lines* represent the target motion starting 300 ms before the beginning of the curve and ending when the target exited the screen. The *solid black lines* depict smooth pursuit behavior during the three trials and the *dashed sections* denote saccades. All the trials are aligned at the position where the target began to curve. Graphs of **c** position, **d** horizontal (*x*) velocity, **e** vertical (*y*) velocity, **f** direction, and **g** speed over time for one trial. The target traversed an angle of $-180°$pa at a radius (*R*) of $1.80°$va, an angular velocity $(\dot\Theta_T)$ of $257°$pa/s and a speed (S_T) of $8.07°$va/s. In this example the target gradually changed direction from 0 to 700 ms

$4.9–11.3°$va/s. The target speed in trials in which direction did not change was chosen at random from the target speeds for curvilinear motion.

The experimental design was such that a particular angular velocity was presented at several radii of curvature. We presented 13 combinations of radius and angular velocity (referred to as conditions, Table 1). In each condition, direction could change by nine angles, and there were seven repeats, for a total of 819 trials. There were few differences in the response to a clockwise and counterclockwise target motion. Thus, for all analyses, angles of the same magnitude, but different directions (positive and negative) were combined (angle $n=5$).

Table 1 Target motion parameters

	Radius °va (cm)				
	1.08 (1.62)	1.80 (2.70)	2.52 (3.78)	3.24 (4.86)	3.96 (5.94)
Angular velocity °pa/s (Speed °va/s)	257 (4.9)	200 (6.3)	150 (6.6)	100 (5.7)	
	300 (5.7)	257 (8.1)	200 (8.8)	150 (8.5)	
	400 (7.5)	300 (9.4)	257 (11.3)	200 (11.3)	150 (10.4)

Perturbation experiments (Experiment 2)

Two females and three males (ages 20–49) volunteered for a second set of experiments, where small perturbations were presented on some trials just before the target began to change direction. Otherwise, target motion was similar to that in Experiment 1. Specifically, the target changed direction by 0, ±130, ±170 and $\pm200°$pa (except as noted). The radii of curvature were 1.80, 2.52 and 3.24°va and the target angular velocities were 150 and 200°pa/s. Every radius of curvature was combined with every angular velocity and each one of these six combinations was termed a target motion condition.

Perturbation and control trials were randomly interleaved. When perturbations occurred, they lasted from -16.67 to 0 ms, with time zero (0 ms) defined as the time when the target began to curve. Three types of perturbations were applied, each in a separate experiment. One affected only target speed, a second affected only target direction, and a third affected both.

In the *Speed Decrease* perturbations, the target stopped briefly just before the curve ($\Delta V_x = -V_o$, $\Delta V_y = 0$). This motion is illustrated schematically in Fig. 9 (red hexagon), where unperturbed target motion is represented with the gray circles. In the *Direction Only* perturbations, the target moved perpendicularly up or down ($\Delta V_x = -V_o$, $\Delta V_y = \pm V_o$). This perturbation (blue and purple squares in Fig. 9a) introduced a step change in direction without affecting speed (Fig. 9b, c). In the *Direction and Speed* perturbations ($\Delta V_x = 0$, $\Delta V_y = \pm V_o$), the target motion was perturbed diagonally at $\pm45°$pa (Fig. 9a, green and orange stars). Accordingly, the direction as well as the speed of the target motion changed, speed increasing by a factor of $\sqrt{2}$ (Fig. 9b, c). In the *Speed Decrease* and *Direction and Speed* experiments, target motion could curve in either direction; in the *Direction Only* experiments the curve was always upwards. There were five repeats of the six target motion conditions at seven angles (four angles for the *Direction Only* experiment) and three perturbation conditions (two for the *Speed Decrease* experiment). Since the final angle should not influence the response to the perturbation, response averages were obtained by combining data for all angles (upward or downward) at each target motion condition.

Data analysis

Using custom software, x- and y-gaze positions for each eye were averaged (to improve the signal to noise ratio) and then differentiated to obtain x- and y-velocity (Vx and Vy). Velocity was filtered with a two-sided exponential filter (time constant of 4 ms; 40 Hz low-pass). Saccades were located using procedures originally developed by Barnes (1982) and subsequently refined by others (Bennett and Barnes 2004; Engel et al. 1999). We first found the time when the gaze speed peaked at a value greater than two times the target speed. The precise starting and ending times of each saccade were then determined from gaze acceleration. The onset of each saccade was found by using an acceleration threshold. The threshold was defined as the average absolute acceleration $+1$ standard deviation taken 80–40 ms before the peak in speed. The time the saccade ended was found in using the same procedures. The beginning and ending times of each saccade were then visually inspected (Mrotek et al. 2004). The saccades were removed from the horizontal and vertical gaze velocities by interpolation with a cubic spline function.

After the desaccading process was completed the absolute peak gaze acceleration for each trial was less than $1{,}000°/\mathrm{s}^2$ (Bennet and Barnes 2004). This procedure identifies saccades smaller than 0.4°va, average saccade amplitude being 1.4°va. These values are similar to those reported by others (Bennett and Barnes 2003, 2004).

Gaze speed (S_g) and direction (Θ_g) were calculated using the desaccaded velocities. Then, direction was differentiated to obtain angular velocity ($\dot{\Theta}_g$). Acceleration was calculated in local path coordinates:

$$A_g = A_{\|g} \times \hat{t} + A_{\perp g} \times \hat{n}, \tag{2}$$

where $\hat{t}$ and $\hat{n}$ are unit vectors tangent and normal to the path. In this description,

$$A_{\|g} = \dot{S}_g, \tag{3}$$
$$A_{\perp g} = S_g \times \dot{\Theta}_g. \tag{4}$$

and $\dot{S}_g$ was obtained by numerical differentiation of S_g.

Results for trials in each condition were averaged after being aligned on the time when the target direction changed. Subsequent data analysis, including statistical analysis (t tests, ANOVAs, linear regression), was performed on the condition averages.

To compute the latency for the change in direction of smooth pursuit, we first found the first peak in angular velocity and fitted a straight line to the points at which pursuit angular velocity was 25 and 75% of the peak value. The zero intercept of this line defined the onset of the response to the curve.

Image velocity

To examine the influence of the retinal slip signal on pursuit, we calculated image velocity in the directions parallel and perpendicular to the instantaneous direction of pursuit. To do so, we first calculated horizontal and vertical image velocities ($V_{x(\mathrm{im})}$ and $V_{y(\mathrm{im})}$) by subtracting the gaze velocity from the target velocity. We then calculated the image direction (Θ_{im}) and image speed (S_{im}) from the horizontal and vertical image velocities;

$$S_{\mathrm{im}} = \sqrt{\left(V_{x(\mathrm{im})}\right)^2 + \left(V_{y(\mathrm{im})}\right)^2}, \tag{5}$$

$$\Theta_{\mathrm{im}} = \left(\tan^{-1}\frac{V_{x(\mathrm{im})}}{V_{y(\mathrm{im})}}\right) - \Theta_g. \tag{6}$$

Finally, we calculated the image velocity along the directions perpendicular and parallel to the instantaneous gaze direction;

$$V_{\parallel im} = V_{x(im)} \times \sin \Theta_g - V_{y(im)} \times \cos \Theta_g, \qquad (7)$$
$$V_{\perp im} = V_{x(im)} \times \cos \Theta_g + V_{y(im)} \times \sin \Theta_g. \qquad (8)$$

In quantitative models of 1D smooth pursuit (Lisberger et al. 1987; Krauzlis and Lisberger 1994a; Churchland and Lisberger 2001), gaze acceleration has been related to image acceleration, velocity and position components, the term proportional to image velocity being the most heavily weighted. In the simplest extension of these models to 2D, the perpendicular and tangential components of gaze acceleration would be related to the respective components of image velocity by a gain factor $\left(G_{\perp im} \text{ and } G_{\parallel im}\right)$. Using Eqs. 3 and 4 we obtain

$$A_{\perp g}(t) = \dot{\Theta}_g(t) \times S_g(t) = G_{\perp im} V_{\perp im}, \qquad (9)$$
$$A_{\parallel g}(t) = \dot{S}_g(t) = G_{\parallel im} V_{\parallel im}. \qquad (10)$$

We tested this model using cross-correlation analysis. To reduce the amount of variability in the data we first filtered gaze acceleration and image velocity with a 10 Hz low-pass filter. We found the time delay that gave the highest correlation and then computed the gains $\left(G_{\perp im} \text{ and } G_{\parallel im}\right)$ from the slopes of the regression.

Image velocity difference

For the perturbation experiments, we examined the response to the perturbation alone by finding the difference between the image velocity in control and perturbation trials. To compute the image velocity difference, we subtracted the horizontal and vertical image velocity response during control conditions from the response during the perturbation conditions

$$\Delta V_{x(im)} = V_{x(im)perturbation} - V_{x(im)control} \qquad (11)$$
$$\Delta_{y(im)} = V_{y(im)perturbation} - V_{y(im)control}. \qquad (12)$$

We used the horizontal and vertical image velocity difference measures to calculate components along directions parallel and perpendicular to the direction of smooth pursuit (see Eqs. 7, 8) and then computed the gain of the response to the perturbation in the directions perpendicular and parallel to gaze direction (Eqs. 9, 10).

Results

In the first experiment we asked subjects to track a small target that initially moved horizontally across a screen, then gradually changed direction by moving in a circular arc, and then moved in a straight line again (Fig. 1a). The radius of curvature of the arc, the target's angular velocity and the amount by which direction changed varied unpredictably from trial to trial (Table 1).

Tracking a target moving circularly

Subjects accurately tracked the target prior to the curve. After the target motion began to curve, smooth pursuit began to change direction and then a saccade reduced the position error. Figure 1b shows data from three illustrative trials for one subject, aligned on the position where the curve started. Target position is represented with the thin gray lines, smooth pursuit with the black lines, and saccades with the thick, dashed lines. Note that smooth pursuit comprised the majority of the tracking prior to the direction change. After the curve began, the saccadic latency (286 ± 81 ms) was longer than the latency at which smooth pursuit began to change direction (94 ± 34 ms) according to a t test on the condition averages (5 subjects, 8 directions, 13 conditions): $t(518) = 52.678$, $P < 0.001$.

Figure 1c–g presents a description of the temporal evolution of tracking behavior in a trial where target direction changed by 180°pa in the clockwise (negative) direction (Fig. 1c). The horizontal (Fig. 1d) and vertical (Fig. 1e) velocities, and the direction (Fig. 1f) and speed (Fig. 1g) profiles are also shown. Prior to the curve, the target was tracked with a speed gain that was close to one ($S_T = 8.07°$va/s). During the curve, which began at time zero, the horizontal and vertical components of target velocity (Fig. 1d, e) were modulated sinusoidally at frequencies that ranged from 0.28 Hz ($\dot{\Theta}_T = 100$ deg pa/s) to 1.11 Hz ($\dot{\Theta}_T = 400$ deg pa/s). The horizontal and vertical components of gaze velocity changed in a manner that paralleled the changes in target velocity with a delay that is obvious in Fig. 1e. In this particular trial, it appears that the horizontal gaze velocity (Fig. 1d) began changing before the vertical gaze velocity (Fig. 1e); however on an average, this was not the case. Given the experimental design, target direction changed linearly (Fig. 1f), while speed remained constant (Fig. 1g). Changes in pursuit direction paralleled changes in target direction with a delay (Fig. 1f). Just after the curve began, there was a small transient decrease in speed (approximately 100 ms prior to the first saccade).

In the following sections, we will describe changes in the direction and speed of smooth pursuit tracking in more detail, using averaged data aligned on the onset of circular motion.

Changes in pursuit direction

Pursuit direction during the curve revealed a stereotypical response. Figure 2 (left column) shows direction pooled across all subjects and all radii for each angle, and for angular velocities of 150°pa/s (Fig. 2a) and 200°pa/s (Fig. 2c). The right column of Fig. 2 shows the target and pursuit angular velocity (the time derivative of direction) for the average of the largest angles ($\pm 240°$pa).

The initial pursuit direction began to change at a faster rate than the target direction. In Fig. 2a, c, it is apparent that the slope of the pursuit direction trace is steeper than the slope of the target direction line from about 200 to 350 ms. This is manifested as a transient overshoot in angular velocity at about 200 ms (Fig. 2b, d). Following this initial transient, steady state pursuit angular velocity was about the same as target angular velocity. In the left column of Fig. 2, on average, all the gaze direction lines have the same slope as the target line over the interval from 500 to 1,000 ms. In the right column this is shown with the pursuit angular velocity oscillating around the target angular velocity.

The size of the transient overshoot in pursuit angular velocity depended on the parameters of the target motion. We computed the peak angular velocity during the first 300 ms of the target's curve. These values were then normalized as the percent angular velocity overshoot (AVO%),

$$\text{AVO\%} = \left(\frac{\dot{\Theta}_{\text{g.peak}} - \dot{\Theta}_{\text{T}}}{\dot{\Theta}_{\text{T}}} \right) \times 100. \tag{13}$$

The average AVO% across all conditions was $102 \pm 103\%$. According to an ANOVA on the condition averages using radius of curvature and angular velocity as factors, the percent overshoot depended on both of these factors (radius $F_{(4,514)} = 34.362$, $P < 0.001$ and angular velocity $F_{(5,513)} = 93.118$, $P < 0.001$). This trend is shown in Fig. 3, using the average results from all subjects. For the purpose of this illustration, the average AVO% values at each experimental condition (denoted with black dots) were interpolated with a spline (Matlab 6.0; interp1.m). As target angular velocity increased, the AVO% decreased (from 275 to 15%). This could occur

if the peak pursuit angular velocity was constant; however, this was not the case. The peak angular velocity was on an average 632 ± 138°pa/s, but also depended on the radius of curvature and target angular velocity (radius $F_{(4,514)} = 58.542$, $P < 0.001$ and angular velocity $F_{(5,513)} = 53.798$, $P < 0.001$).

After the initial overshoot, the pursuit angular velocity oscillated around the target angular velocity for the remainder of the curve (from about 500 ms to the end; Fig. 2 right column). Average pursuit angular velocity was computed over the last 300 ms of the curve (excluding conditions where the curve lasted for less than 600 ms). It was strongly related to the target angular velocity ($r = 0.918$, Fig. 4); the line of best fit had a slope that did not differ from one (1.014 ± 0.024) and an intercept that did not differ from zero (-4.57 ± 5.20). A forward stepwise regression procedure showed that pursuit angular velocity was not influenced by target radius or speed.

The initial steep change in pursuit direction made up for some of the direction lag that was due to the sensorimotor delay (Fig. 2, left column). Nevertheless, pursuit direction consistently lagged target direction. This was true even for the largest changes in direction (240°pa), as shown schematically in Fig. 5a. In this graph, the arrows denote the average direction of pursuit angular velocity in 40 ms bins. To examine the difference between target and pursuit direction quantitatively, we calculated a direction lag at each point by finding the time at which the direction of target motion most closely approximated the current direction of smooth pursuit. The direction lag increased linearly from the beginning of the curve until approximately 100–120 ms (the sensorimotor delay; Fig. 5b). Thereafter, the slope of the direction lag line began to decrease,

Fig. 2 The average direction (*left column*) and angular velocity (*right column*) of smooth pursuit over time computed for all subjects and radii and two angular velocities [150°pa/s in (**a**) and (**b**); 200°pa/s in (**c**) and (**d**)]. In the *left column* the *thick lines* depict the direction of smooth pursuit for angles Θ_T ranging from 60°pa (*light gray*) to 240°pa (*black*). Results for clockwise target motion have been inverted and then averaged with the data from counterclockwise motion. The right columns depict target and pursuit angular velocity for the largest angle (240°pa), the width of the hatching equaling the 95% confidence interval
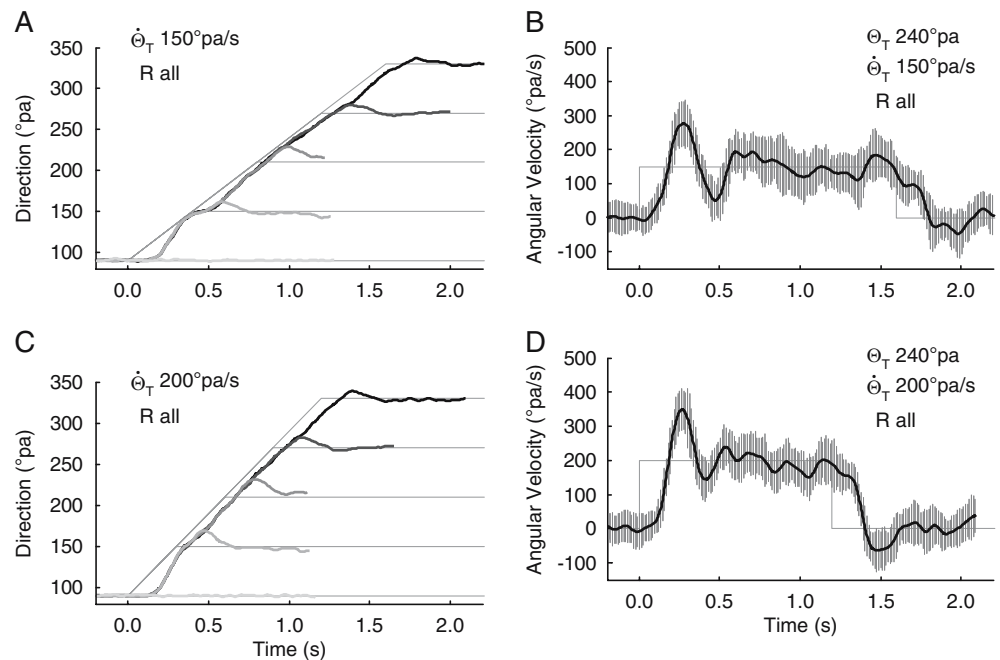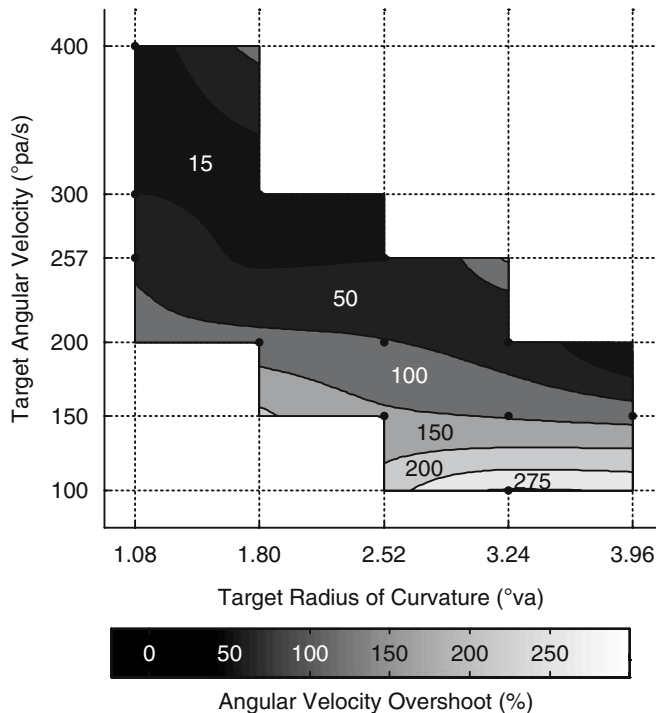
Fig. 3 Dependence of the normalized pursuit angular velocity overshoot ($AVO\%$) on the radius of curvature and angular velocity of target motion. The *black dots* represent the measured values (averages for all angles, subjects and conditions) which were interpolated using a cubic spline algorithm. The scale is shown at the *bottom* of the graph

velocity and radius of curvature (Fig. 6a). Larger radii and faster angular velocities elicited a larger speed decrease (radius $F_{(4,444)} = 7.884$, $P < 0.001$ and angular velocity $F_{(5,443)} = 7.162$, $P < 0.001$). Since the product of the target radius of curvature and angular velocity equals target speed (Eq. 1), the amount by which tracking speed decreased was also proportional to the target's speed ($r = 0.568$, intercept $= 0.33 \pm 0.16$; slope $= 0.010 \pm 0.001$). After normalizing the gaze speed to target speed (Fig. 6b), *Speed Gain* no longer depended on the radius of curvature ($F_{(4,444)} = 2.305$, $P = 0.058$) but it still depended on the target angular velocity ($F_{(5,443)} = 7.114$, $P < 0.001$). The fastest target angular velocity led to a larger decrease in *Speed Gain* compared to all other angular velocities. Furthermore, the decrease in *Speed Gain* only depended weakly on target speed ($r = 0.107$). In general the parameters of the stimulus, especially target angular velocity, influenced the magnitude of the speed decrease. As will be shown in the next section, the decrease in speed could be accounted for by the image motion parallel to the direction of smooth pursuit.

indicating that pursuit started to change direction. The lag reached a minimum at about 400 ms (Fig. 5b), reflecting the overshoot in angular velocity (Fig. 2b, d). Thereafter, the lag oscillated at a constant value of about 80 ms for the remainder of the curve (Fig. 5b).

Pursuit direction lagged behind the target direction for all the conditions. Beyond the initial minimum, it rarely, even briefly, fell to a level near zero. Across all conditions the average direction lag for the last 100 ms of the curve was 82 ± 50 ms, and this value did not depend on any of the parameters of target motion (ANOVA on condition averages with radius, angular velocity and angle as factors, $P > 0.05$). Thus, even though the subjects overshot and then matched the target angular velocity, they did not catch up to the direction of the target.

Modulations in pursuit speed

During the initial segment of the trial (horizontal target motion), pursuit speed was very close to target speed. In fact, the normalized speed (*speed gain*) for the 200 ms before the beginning of the curve was 0.95 ± 0.05 (for all subjects, conditions and angles).

After the target began to change direction, pursuit speed decreased transiently over the course of several hundred ($\sim$500) milliseconds (Fig. 5c). The magnitude of this decrease depended on the target's angular

Correlation between image velocity and smooth pursuit acceleration

As mentioned in the Introduction, feedback models in which eye acceleration during tracking is driven by error signals related to retinal slip (i.e., retinal image motion) have successfully accounted for the response to target motion in 1D (Churchland and Lisberger 2001; Krauzlis and Lisberger 1994a; Lisberger et al. 1987). Specifically, the eye acceleration output is related to retinal image position, velocity and acceleration inputs, with image velocity providing the dominant contribution. To interpret the direction and speed responses in the present experiments, we computed retinal image motion and decomposed the image signal and the gaze response into two components, one parallel and the other perpendicular to the instantaneous direction of smooth pursuit (Eqs. 7, 8, 9, 10).

According to the image motion models, horizontal and vertical pursuit acceleration should be related to horizontal and vertical image velocity. In our experiments, the horizontal and vertical components of target velocity were modulated sinusoidally, and as described previously, to a first approximation, pursuit velocity followed, but lagged the target motion (Fig. 1d, e). The x- and y-components of image velocity also appear to be modulated sinusoidally (Fig. 7a, b), with the x-image velocity following a sine wave and the y-component resembling a cosine function.

As shown in Fig. 7c, d, the component of image velocity perpendicular to the direction of smooth pursuit was much larger than the component that paralleled the direction of smooth pursuit. Maintaining the reasoning of the image motion models described earlier, one would expect the perpendicular and parallel components of
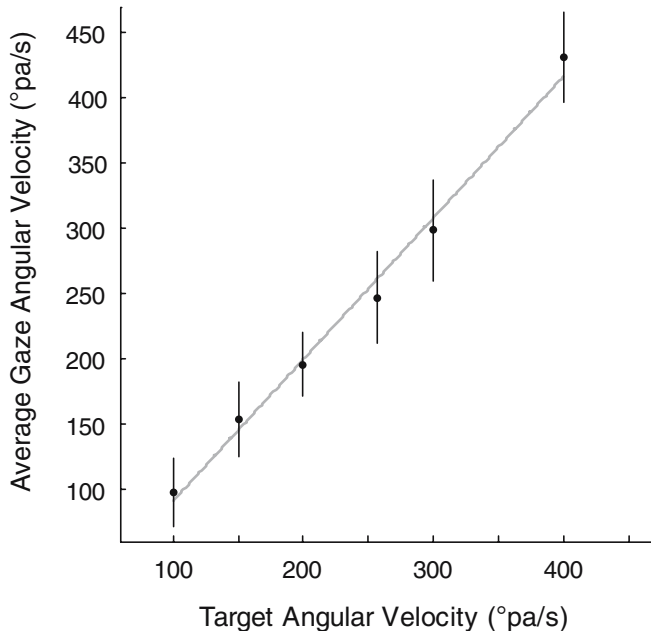
Fig. 4 Relation between steady state gaze angular velocity and target angular velocity. The average pursuit angular velocity was computed over the last 300 ms of the curve for all conditions that lasted longer than 600 ms. *Error bars* represent ± 1 standard deviation from the mean and the *gray line* is the line of best fit. Data from all subjects and conditions from Experiment 1 are shown. The relationship was linear with a slope of 1.01 ± 0.02 and an intercept of $-4.57 \pm 5.2°/$s

gaze acceleration $\left(A_{\perp g} A_{\parallel g}\right)$ to be correlated with the respective components of image velocity $(V_{\perp im}, V_{\parallel im})$. $A_{\perp g}$ is equal to the product of the pursuit angular velocity and speed (Eq. 9). Since gaze speed changed little during the trials, one would expect $V_{\perp im}$ to resemble pursuit angular velocity. In fact, $V_{\perp im}$ in Fig. 7c shows a strong resemblance to pursuit angular velocity (Fig. 2b, d).

Following the same logic, the $A_{\parallel g}$ should be proportional to the $V_{\parallel im}$ (Eq. 10). In general, the pursuit speed changes were small during the time the target followed a circular arc, most noticeably decreasing shortly after the target began to change direction. Since speed changed little, its time derivative, $A_{\parallel g}$, was close to zero. The $V_{\parallel im}$ was also close to zero throughout the curve (Fig. 7d), with a small negative transient beginning at time zero.

The gain of the relationships between the two components of gaze acceleration and the two components of image velocity were computed using a cross-correlation analysis. We first calculated the lag magnitude using cross-correlation analysis and set the lead/lag maxima at 200 ms. If a condition was computed to have the lead/lag at this maximal value, it was removed from future analyses. There were 520 conditions and 64 were removed for this reason, for a final total of 456 conditions. The gain of the response was then computed by linear regression between the response and the shifted input. Typical results are illustrated for one experimental condition in Fig. 8. As was generally the case, there was a

good correspondence between $V_{\perp im}$ and $A_{\perp g}$ (Fig. 8a, b). In this example, the $V_{\perp im}$ led the $A_{\perp g}$ by 100 ms (the average of all conditions was 89 ms; Table 2). The shifted $A_{\perp g}$ values are graphed against the $V_{\perp im}$ values in Fig. 8b. The points lie close to a line with a slope of 10.2/s. The correlation between $V_{\parallel im}$ and $A_{\parallel g}$ was not as strong, one possible reason being that the $V_{\parallel im}$ was small throughout the curve (compare Fig. 8d with b). However, some similarities between $V_{\parallel im}$ and $A_{\parallel g}$ are apparent in Fig. 8c. Both the profiles have a small initial decrease and, then a quick rise and fall. For this example, the $A_{\parallel g}$ lagged $V_{\parallel im}$ by 68 ms and the gain was 3.8 s^{-1} (Fig. 8d).

A quantitative analysis showed that there was a good correlation between the two components of gaze acceleration and the respective components of image velocity (Table 2). In this analysis, we used the averaged data for each subject and each experimental condition. The correlation between $A_{\perp g}$ and $V_{\perp im}$ was stronger (0.85) than the correlation between $A_{\parallel g}$ and $V_{\parallel im}$ (0.64). The average time delays (89 and 74 ms, respectively) are in line with our other estimate of the time delay (94 ms). Finally, this analysis suggested that smooth pursuit gain was larger in the perpendicular direction (9.8 s^{-1}) than it was in the tangential direction (5.7 s^{-1}). Using a paired t test across all conditions, we found these gain factors differed significantly ($t_{(455)} = 24.548$, $P < 0.001$).

The gains for each condition were also examined individually by comparing the two gains, taking into account the uncertainty in the slopes of the regressions. In 77% (352/456) of the conditions the gain was larger ($P < 0.05$) in the perpendicular direction compared to the parallel direction. In only 5% (22/456) of conditions the gain in the parallel direction was larger than in the perpendicular direction. In the remaining 18% (82/456) of the conditions the perpendicular and parallel gains were statistically the same.

Influence of perturbations on tracking of circularly moving targets

To more directly test directional asymmetries in the gain of smooth pursuit, in a second set of experiments we applied brief perturbations timed to the onset of the curvilinear target motion. Subjects reported that they did not always notice the perturbations, nor could they accurately describe their characteristics. Furthermore, the likelihood of a perturbation ($\geq 50\%$) did not affect tracking behavior in control trials, where no perturbations were applied. This was ascertained by comparing the results of the second set of experiments to those obtained in the first, where there were no perturbations. Pursuit direction and the normalized pursuit speed in the interval 200 ms before the onset of the curve were not appreciably influenced ($< 3\%$) by the likelihood of a perturbation (Table 3). The average direction and average normalized speed of smooth pursuit for the time period from 200 to 400 ms after the onset of the curve were also unaffected.
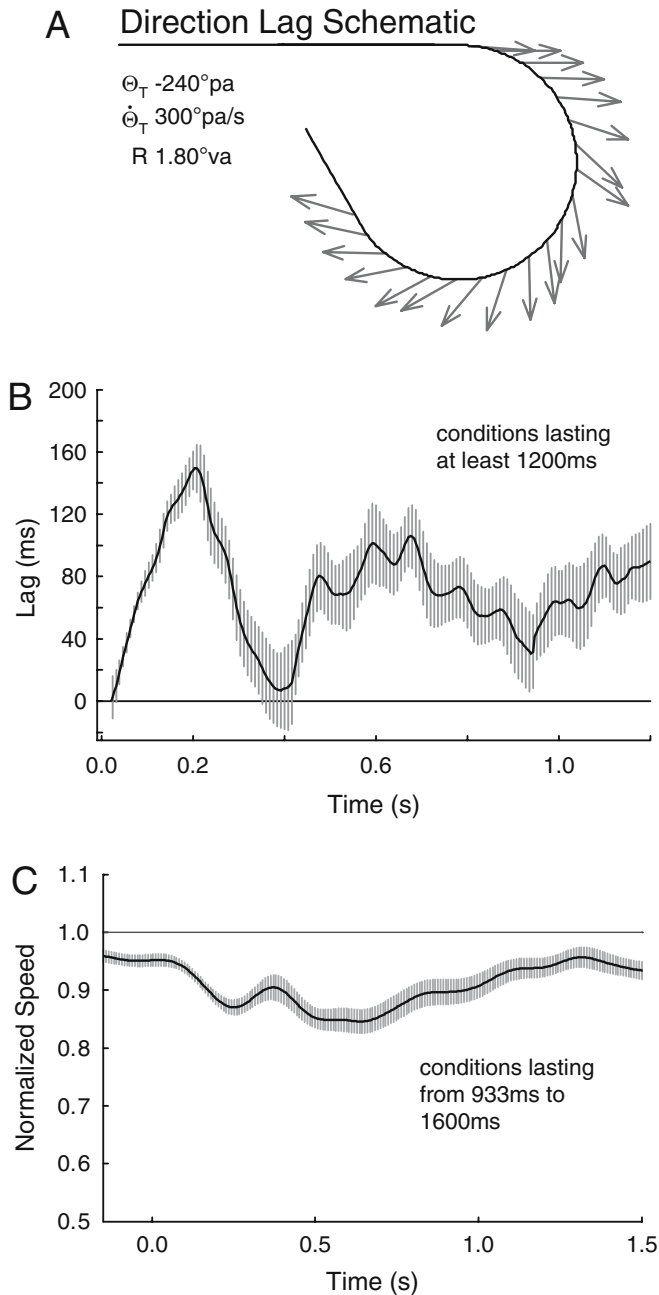
Fig. 5 Lag of pursuit direction relative to the direction of target motion and variation in pursuit speed. **a** Shows a schematic of lag in the pursuit direction relative to the target direction grouped at 40 ms intervals. Each *arrow* begins at the target position at the center of the bin and points in the direction of pursuit for that bin. The data are for one condition (1.80°va radius and 300°pa/s angular velocity) and one angle, and one subject. **b** Shows direction lag during circular target motion for all subjects and angles in conditions where the target curved for at least 1,200 ms. *Positive values* indicate that the gaze direction is behind the target direction. The width of the hatching is equal to the 95% confidence interval. **c** Variation in normalized pursuit speed during circular target motion. The trace shows data averaged over all subjects, radii, and angular velocities ranging from 150 to 257°pa/s and the largest angle (±240°pa). Pursuit speed has been normalized to the target speed and the width of the hatching is equal to the 95% confidence interval. Note the gradual decline in pursuit speed during the curve (all curves began at 0 ms and lasted more than 900 ms)
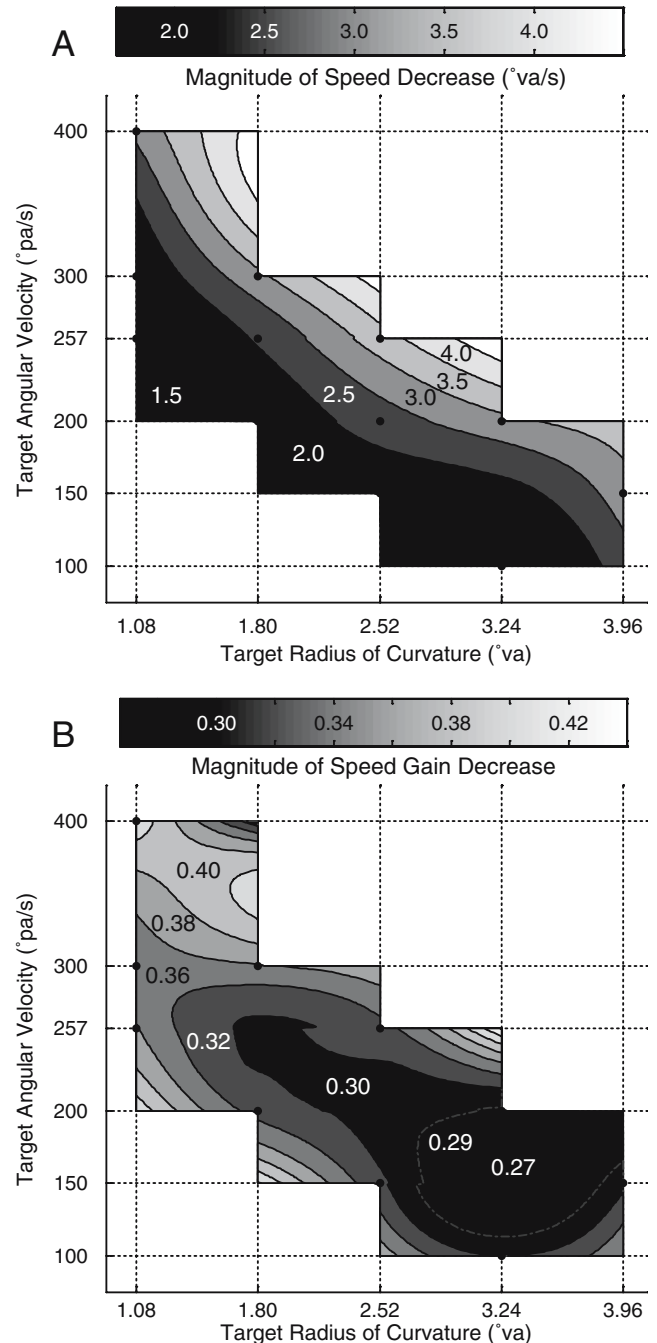

Fig. 6 Dependence of the speed of smooth pursuit on target radius of curvature and angular velocity. **a** Shows a contour graph of the magnitude of the decrease in speed for all conditions and **b** shows the same data after speed was normalized to target speed. The *black dots* denote measured values which were interpolated and extrapolated with a cubic spline algorithm

We computed the response to the perturbation by subtracting the response in control trials from the responses in trials (with the same target curve characteristics) in which there was a perturbation. Our subsequent analysis was based on the assumption that responses to the perturbation and to the unperturbed target motion added linearly, i.e., the tracking of the curve was not

Fig. 7 Retinal image motion during tracking of a circularly moving target. The panels depict averaged data from all subjects, all radii and one angle magnitude (±240°pa), and one angular velocity (257°pa/s), the hatching denoting 95% confidence intervals. Image velocity is depicted in two different coordinate systems: Cartesian (**a** and **b**) and local path coordinates (**c** perpendicular and **d** parallel)
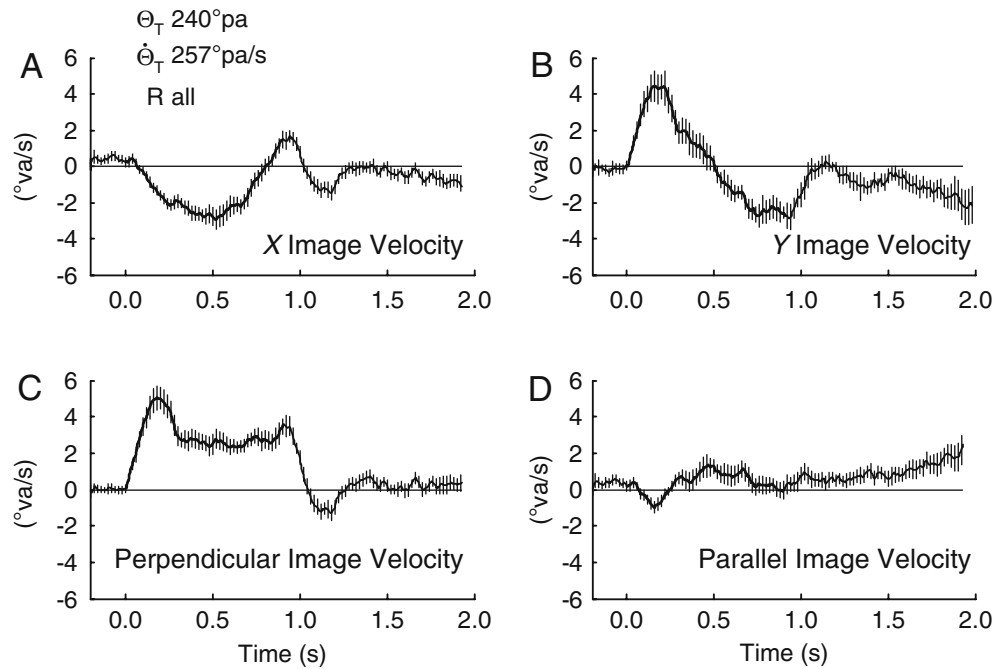

Fig. 8 Correspondence between image velocity and gaze acceleration. Both parameters are defined in local path coordinates: perpendicular to the instantaneous direction of smooth pursuit (**a** and **b**) and parallel to this direction (**c** and **d**). The traces depict averaged values for one angle (±180°pa) and one angular velocity (200°pa/s) for all subjects and radii. Traces in the *left panels* were obtained by normalizing results for each condition to its maximal value before averaging. Gaze acceleration in the two directions (**a** perpendicular, $A_{\perp g}$; **b** parallel, $A_{\parallel g}$) is shown at the time it occurred (*dashed gray*) and shifted earlier (*solid gray*). The correlation between image velocity and the shifted gaze acceleration is $r = 0.96$ (**a**) and 0.58 (**c**). Panels **b** and **d** illustrate differences in the gain (slope of gaze acceleration vs. image velocity) in the two directions. In **b** the line of best fit had a slope of 10.2 and an intercept of 3.4. In the parallel direction (**d**), the gain was much lower (slope of 3.8 with an intercept of −3.1)
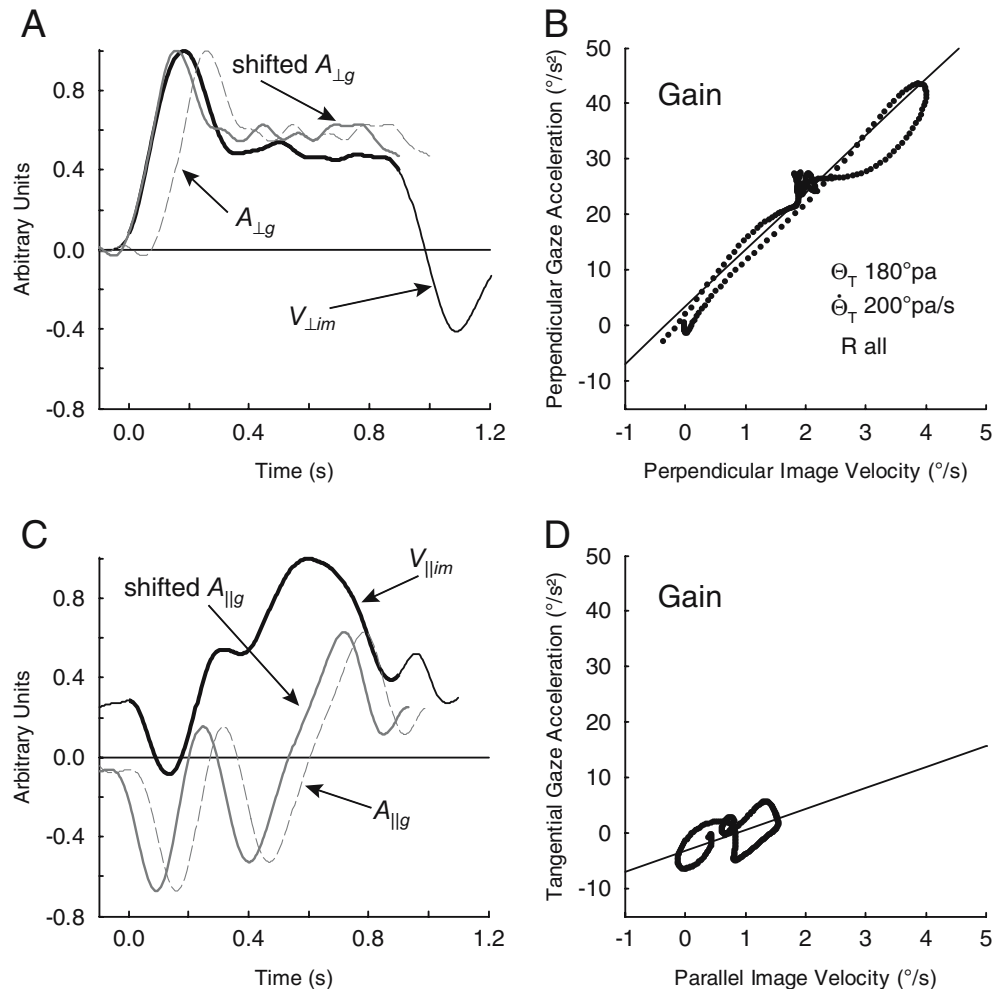
Table 2 Pursuit gain

	Coefficient of determination	Gain (S^{-1})	Lag (ms)
$V_{\perp\text{lim}}$ with $A_{\perp\text{g}}$	0.85 ± 0.09	9.78 ± 1.79	89 ± 19
$V_{\|\text{lim}}$ with $A_{\|\text{g}}$	0.64 ± 0.19	5.73 ± 3.08	74 ± 34

affected by the perturbation. If the assumption is correct, the responses to perturbations should be the same in trials where the target curved and in trials where the target continued on a straight line.

We performed a statistical comparison on the peak change in speed (ΔS) and the peak change in direction ($\Delta \Theta$) in the condition averages attributable to the perturbations. Statistically, ΔS was different for target motion conditions with and without gradual changes in direction ($F_{(1,868)} = 12.637$, $P < 0.001$). This effect was only present for the Up and Faster and Down and Faster perturbations (stars in Fig. 9a), the ΔS being about 25% smaller when the target continued in a straight line. The peak $\Delta \Theta$ was the same for target motion conditions with and without curves ($F_{(1,868)} = 0.785$, $P = 0.376$). Overall, the responses to perturbations in conditions with and without curves had similar profiles (data not shown) and magnitudes. Therefore, with the exception noted above, our analysis supports the hypothesis that the response to the curve and the response to the perturbation were independent.

Pursuit direction and speed responses to perturbations

The effects of the various perturbations illustrated in Fig. 9 on the direction and speed of smooth pursuit are depicted in Figs. 10 and 11. Changes in the direction of the target's motion and gaze are shown in the left column of Fig. 10, the straight solid gray lines representing the target motion and the curved black lines representing the pursuit direction for the control trials. The colored lines represent the gaze direction for the trials with perturbations. The right panels of Fig. 10 illustrate the effect of each of the perturbations; they were obtained by subtracting results from control trials from those for trials with perturbations. The direction of the subsequent curve did not affect the magnitude of the response to the perturbations (*Direction and Speed experiment*, Speed: $F_{(1,358)} = 0.652$, $P = 0.42$; Direction: $F_{(1,358)} = 0.232$, $P = 0.631$). Therefore, in Fig. 10 we have combined the responses to each of the perturbations from all trials, irrespective of the direction of the subsequent curve.

The direction of smooth pursuit was unaffected when the target's motion stopped transiently (*Speed Decrease*, Fig. 10a, b). In comparison, a perturbation in target direction (and speed) did affect the direction of smooth pursuit, with gaze direction increasing faster when the target's motion was perturbed upward, and increasing more slowly when the target's motion was perturbed downward (Fig. 10e, f). However, the responses to the *Direction Only* perturbations were asymmetrical, as shown in Fig. 10c, d. It should be noted that in the *Direction Only* experiment, the target always curved counterclockwise, whereas there was equal probability of clockwise and counterclockwise curves in the other experiments. We suspect that this led to an upward bias in the expectation of target motion in the *Direction Only* experiment and that the asymmetry in the response gain reflected the asymmetry in expectation. The directional perturbations in target motion led to a response starting after 100 ms and lasting for almost 200 ms. The response consisted of an initial large change in the direction of motion ($\sim$15°pa), with a transient overshoot, followed by a plateau and a gradual decline to zero.

Changes in the speed of smooth pursuit in response to the perturbations are shown in Fig. 11. In all trials with perturbations (colored lines), pursuit speed decreased rapidly at a latency of 90 ms after the perturbation, reaching a minimum at approximately 150 ms. The transient speed decrease was finished by 350 ms. This response was especially unexpected in the *Direction and*

Table 3 Gaze direction and speed comparisons before and during curve

	Before the curve		During the curve	
	Direction (°pa)	Normalized speed	Direction (°pa)	Normalized speed
Experiment 1[c]	90.22 ± 0.18	0.949 ± 0.012[c]	129.73 ± 3.75	0.880 ± 0.024
SpdCntrl[a]	89.88 ± 0.29	0.977 ± 0.005	125.09 ± 3.52	0.913 ± 0.035
SpdPrt[a]	89.96 ± 0.24	0.975 ± 0.004		
DirCntrl[a, b]	91.97 ± 0.77[b]	0.977 ± 0.010	124.57 ± 3.84	0.916 ± 0.018
DirPert[a, b]	92.00 ± 0.70[b]	0.976 ± 0.010		
DirSpdCntrl[a]	90.23 ± 0.21	0.979 ± 0.009	127.40 ± 3.29	0.901 ± 0.032
DirSpdPrt[a]	90.16 ± 0.13	0.978 ± 0.009		

All values are the mean $\pm$ standard deviation
[a] *SpdCntrl* Control trials in the *Speed Decrease* experiment; *SpdPrt* Speed Decrease perturbation trials; *DirCntrl* control trials in the *Direction Only* experiment; *DirPrt* up only and down only perturbation trials; *DirSpdCntrl* control trials in the *Direction and Speed* experiment; *DirSpdPrt* up and faster and down and faster perturbation trials
[b] Initial tracking direction was 2% more counterclockwise compared to all the other experiments ($F_{(6,28)} = 23.347$, $P < 0.001$)
[c] The normalized speed was 3% lower than the normalized speed in all the other experiments ($F_{(6,28)} = 7.090$, $P < 0.001$)
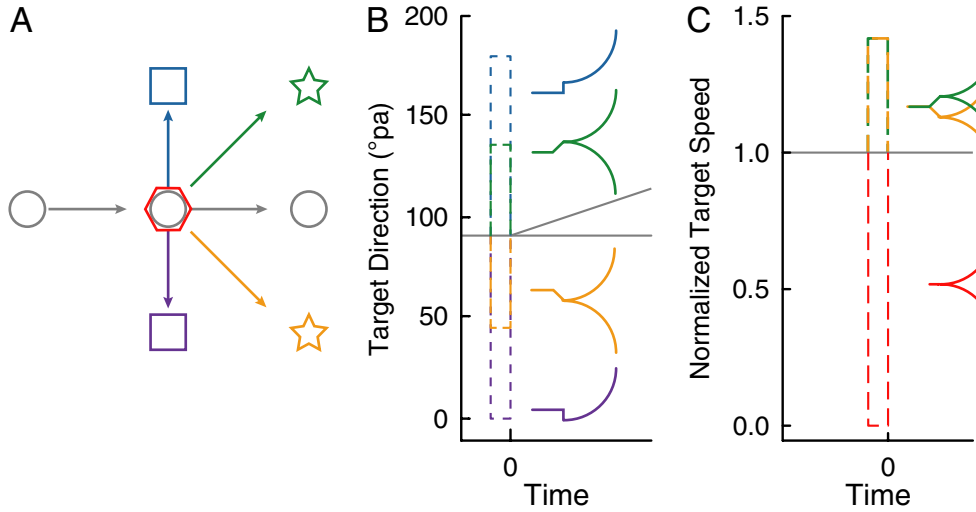
Fig. 9 Schematic illustrating different types of perturbations applied in Experiment 2. Perturbations lasting 16.67 ms were applied at the onset of circular target motion. Their direction is indicated schematically in (**a**) and their effect on the direction and speed of target motion is indicated by the various *colored dashed lines* in (**b**) and (**c**). The control trials are shown with the *gray lines* and each perturbation is denoted by a different *color dashed line*. For the *Speed Decrease* perturbations (*red*), speed decreased to zero transiently but there was no perturbation in target direction. For the *Direction Only* perturbations (*cyan* and *purple*), the target was perturbed 90°pa from the initial direction, with no change in speed. In the *Direction and Speed* perturbations (*green* and *orange*), the target's direction changed by 45°pa from the initial direction and speed increased by a factor of $\sqrt{2}$. The *insets* in (**b**) and (**c**) show the target paths resulting from each of the perturbations. The *color code* denotes the type of perturbation and is consistent in this and following figures

Speed experiment (Fig. 11e, f) because those perturbations led to a transient increase in target speed.

Pursuit response to image motion after perturbations

Changes in image velocity could account for the directional responses to the perturbations (Fig. 10) but they did not entirely account for the speed transients (Fig. 11). Changes in image velocity (ΔV_{im}) were derived by computing the difference between image velocity in the control and perturbation conditions (Eqs. 11, 12).

The average image velocity for each experiment is shown in Fig. 12; the direct effect of the perturbation on image velocity being represented by the fast transient just before time zero. The changes in the direction of smooth pursuit illustrated in the insets (from Fig. 10) are compatible with the changes in $V_{\perp im}$ (Fig. 12; left column). Changes in direction followed the perturbation-induced $\Delta V_{\perp im}$ with a latency close to 100 ms, and in turn gave rise to secondary changes in $\Delta V_{\perp im}$.

In contrast to the results for direction and $\Delta V_{\perp im}$, not all speed differences of smooth pursuit (Fig. 11) can be explained by evoking this image motion mechanism. A negative transient in $\Delta V_{\parallel im}$ around time 0 did lead to a transient decrease in pursuit speed (insets from Fig. 11) for the *Speed Decrease* and *Direction Only* perturbations (Fig. 12b, d). However, in the third experiment (*Direction and Speed* perturbations, Fig. 12f), speed decreased even though there was no change in $V_{\parallel im}$ prior to 100 ms (the increase in $V_{\parallel im}$ thereafter was a consequence of the decrease in pursuit speed). This suggests that the re-

sponse to a brief perturbation consisted of two distinct components, one that was related to the properties of the perturbation (as reflected in the change in gaze direction) and a second response that was nonspecific, triggered by the perturbation and that led to a transient decrease in speed.

A closer examination of the speed profiles in Fig. 11 (and the insets in Fig. 12) suggests that this explanation is reasonable. Speed decreased more (in Fig. 11b, d) when there was a transient decrease in $V_{\parallel im}$ (Fig. 12b, d) than when there was not (Figs. 11f, 12f). The difference in responses to these perturbations can be most readily appreciated by comparing the changes in gaze velocity in Cartesian coordinates (Fig. 13). In this coordinate system, the *Speed Decrease* perturbation led to a decrease in x-velocity and no change in y-velocity ($\Delta V_x = -V_o$, $V_y = 0$). For the *Direction Only* perturbation, the perturbation in x-velocity is the same but there is also a perturbation in y-velocity ($\Delta V_y = \pm V_o$). Finally, for the *Direction and Speed* perturbations, $\Delta V_x = 0$. Since motion was initially horizontal, changes in x-velocity (Fig. 13a) resemble the changes in speed shown in Fig. 11, while changes in y-velocity (Fig. 13b) resemble the changes in direction shown in Fig. 10 ($\theta \approx \tan^{-1}(\Delta V_y / V_x) \approx \Delta V_y / V_x$).

In Fig. 13, the colored lines denote the x- and y-velocity components of the responses to a perturbation restricted to the x-direction (*Speed Decrease* perturbation, red line) or to the y-direction (*Direction and Speed* perturbation, green and orange alternating line). The heavy solid line represents the difference between the two. Assuming linear summation of a specific and a

Fig. 10 Effect of perturbations on the direction of smooth pursuit. The *left panels* (**a**, **c** and **e**) show the direction of smooth pursuit averaged over all subjects, radii, positive angles, and one angular velocity (150°pa/s). The *gray line* represents the motion of the target. The *solid black lines* show the direction response for the control conditions, while the *colored lines* show the response for each of the perturbations. The *right panels* (**b**, **d** and **f**) show the difference in direction between perturbed and control trials, obtained by averaging over all angles and all target motion conditions for all subjects. The width of the hatching is equal to the 95% confidence interval. *Color coded* target position schematics are also shown for each perturbation type
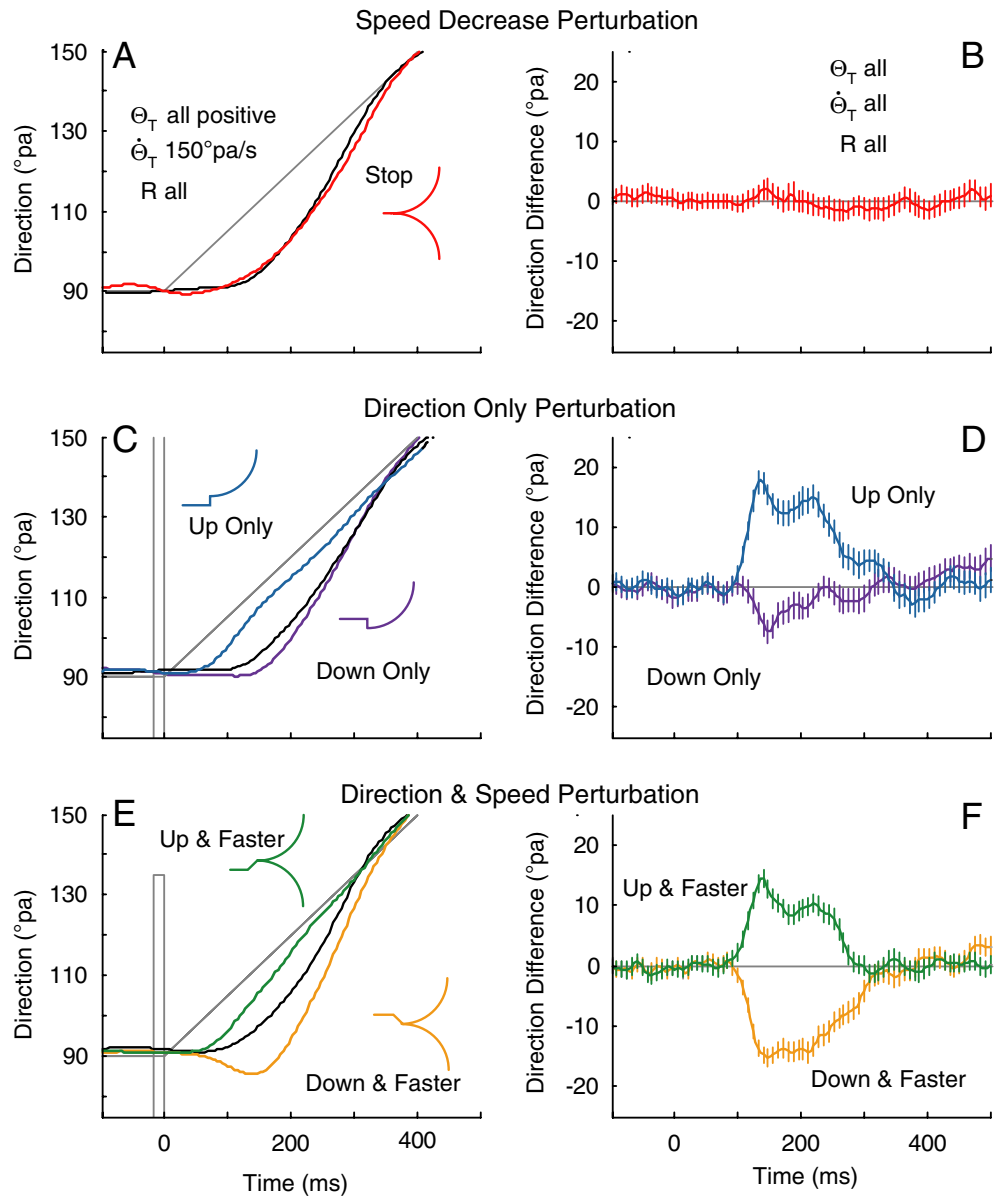
nonspecific response, the results of the subtraction would represent the component specific to the perturbation. Note that the analysis yields a specific response to a perturbation in the *x*-direction (Fig. 13a) that is more transient and has a smaller amplitude than the specific response to a perturbation in the *y*-direction (Fig. 13b). Thus, the gain of the response to a perturbation in the direction away from the initial direction of gaze (*y*-direction) was larger than the gain of the response to the perturbation along the direction of gaze (*x*-direction).

Discussion

We examined the smooth pursuit tracking of targets that initially moved in a straight line and then followed the arc of a circle. The target's trajectory was chosen to more closely approximate pursuit tracking under everyday conditions, such as the tracking of a ball following a parabolic arc. In the present experiments, the target's speed was constant throughout each trial, as was its angular velocity during the curvilinear portion of the trajectory. Therefore, the results of these experiments are context dependent for conditions where subjects are aware of the general form of the target motion (that it was moving in two dimensions; specifically that it began moving horizontally and then it was likely to travel in a circular path). However, as was borne out by the results, crucial details of the target's trajectory, such as the radius of curvature, its angular velocity and the duration of the curve, were unpredictable.

We characterized the speed and direction of smooth pursuit in response to step changes in angular velocity. Even though target motion was predictable in the sense that it always followed a circular path, pursuit direction

Fig. 11 Effect of perturbations on the speed of smooth pursuit. The *left panels* (**a**, **c** and **e**) show the speed response normalized with respect to target speed. Responses on trials with perturbations are shown with the *colored lines*, and for the control conditions with the *black lines*. Profiles are for all subjects, all radii, all upward angles, and one angular velocity (200°pa/s). Panels on the *right* (**b**, **d**, and **f**) depict the effect of the perturbation, obtained by subtracting the speed profile in the control condition from the speed profile in the perturbation condition and averaging over all angles, target motion conditions, and subjects. The width of the hatching represents the 95% confidence interval. *Color coded* target position schematics are also shown for each perturbation type
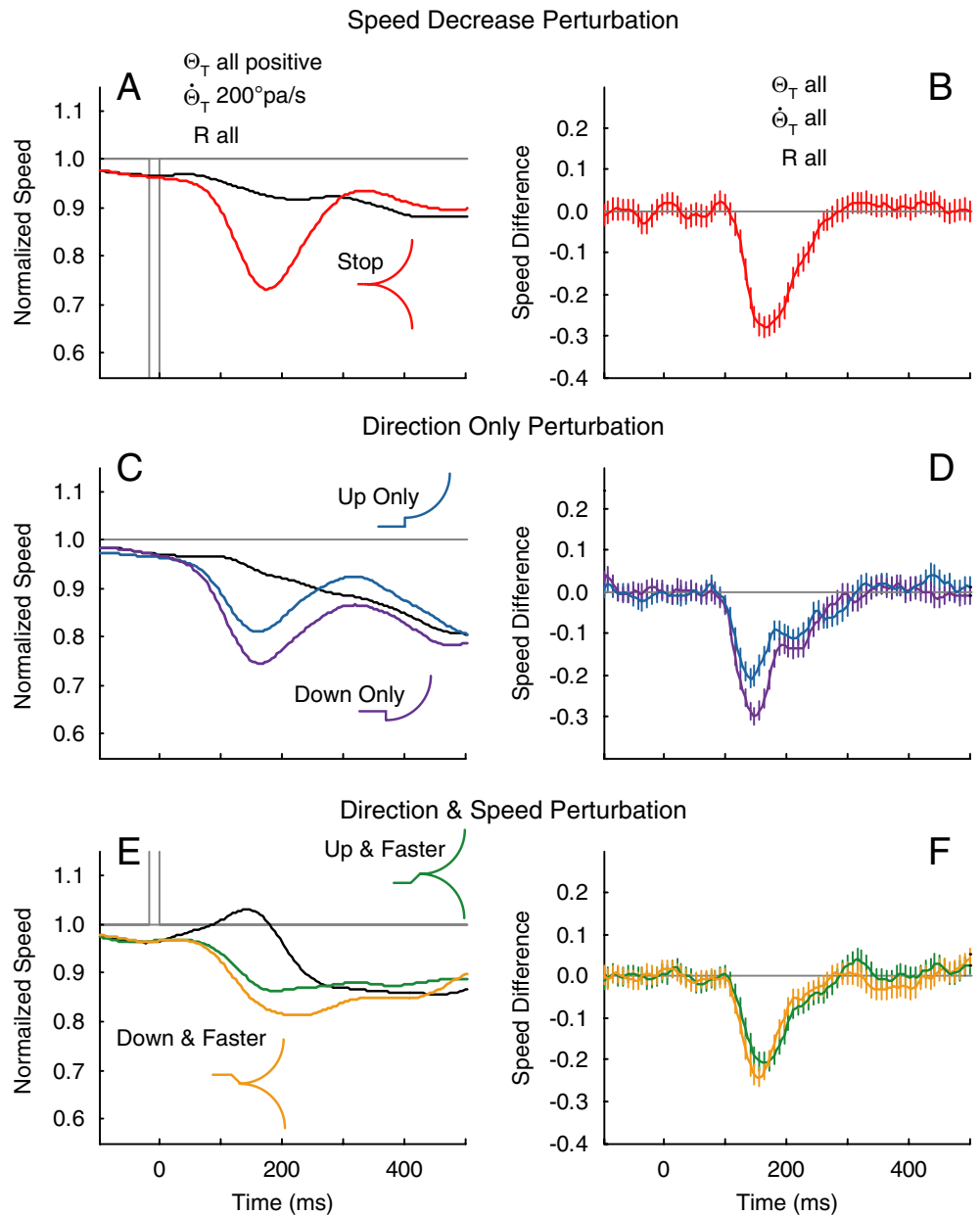

always lagged the target's direction. Accordingly, under these experimental conditions, pursuit was governed primarily by feedback of retinal image motion. In fact, a simple feedback model in which eye acceleration was proportional to image velocity was able to account reasonably well for the time course of the responses. According to this model, pursuit gain was anisotropic, being larger in the direction perpendicular to gaze velocity than in the parallel direction.

Lack of predictive pursuit

During the time that the target followed a circular path, the direction of smooth pursuit consistently lagged the direction of target motion (Figs. 2, 5a, b). Computed

over the last 100 ms of the curve, this lag averaged 82 ms, a value that is close to the latency for the initiation of smooth pursuit (94 ms in the present experiments). This was true even when the circular motion lasted as long as 1.6 s (Fig. 2) or even 2.4 s. This result was surprising because it is well established that subjects can track linear, sinusoidal target motion with lags close to zero (Bahill and McDonald 1983; Barnes et al. 2000; Dallos and Melvill-Jones 1963; Deno et al. 1995). This is true even for fairly complicated 2D trajectories generated from sums of sines (Kettner et al. 1996). Most of those studies dealt with steady state behavior. However, essentially zero lag is attained within one cycle of a predictable sinusoidal motion, i.e., within about 1 s (van den Berg 1988). In the present experiments, a large number of factors were unpredictable from trial to trial.

Fig. 12 Effect of perturbations on the image velocity. Panels in the *left column* (**a**, **c** and **e**) show the change in the perpendicular image velocity in trials with and without perturbations $(\Delta V_{im\perp})$ and the panels in the *right column* (**b**, **d** and **f**) show the same for parallel direction $(\Delta V_{im\parallel})$. Responses are averages from all subjects, angles, and target motion conditions. The width of the hatching represents the 95% confidence interval. For comparison purposes, differences in pursuit direction and speed (from the right columns of Figs. 11, 12) are reproduced in the *inserts*. *Color coded* target position schematics are also shown for each perturbation type
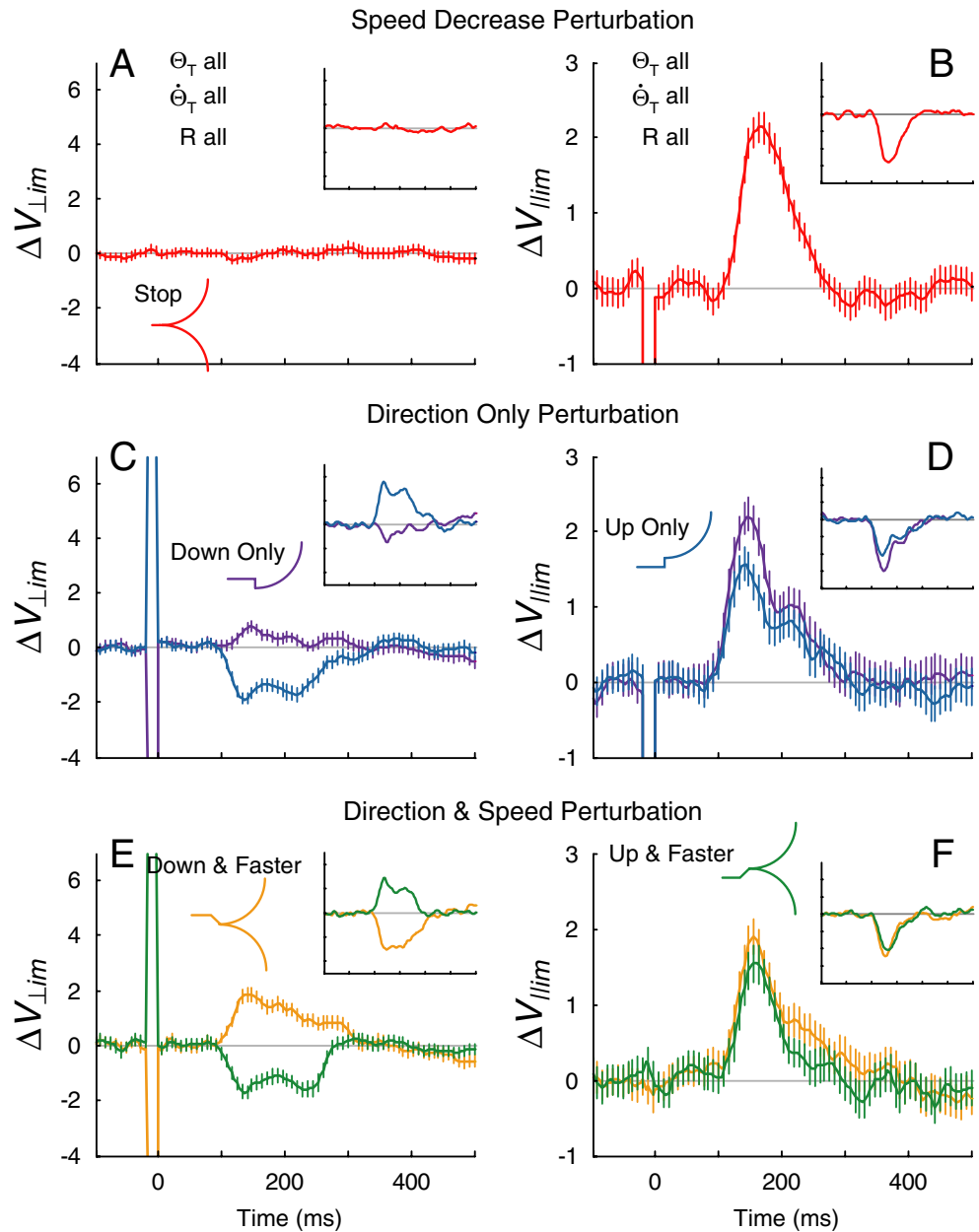
Among these were the target's speed, the radius of the circle, its arc length and the time at which target motion began to curve. Presumably these factors sufficed to prevent predictive tracking, even though subjects were well aware that the motion would almost always be circular.

Path coordinates

Because the stimulus maintained a constant speed and underwent a step change in angular velocity, we found it convenient to characterize the response in terms of speed and direction. Such a parameterization leads naturally to a description of the motion in local path coordinates, i.e., in coordinate axes that are tangent and perpendic-

ular to the instantaneous motion. In this coordinate system, the tangential acceleration is equal to the rate of change in speed, while the perpendicular acceleration is equal to speed times the angular velocity.

For linear target motion, feedback models in which eye acceleration is related to retinal image velocity and its derivative have successfully accounted for a large body of behavior (Churchland and Lisberger 2001; Krauzlis and Lisberger 1994a; Lisberger et al. 1987). Extending the logic of this model to two dimensions, one would expect that the rate of change of pursuit speed would be proportional to image velocity in the direction paralleling the direction of smooth pursuit. Under the present experimental conditions, image velocity in this direction was small (Fig. 7d) and, consistent with our premise, speed changed gradually and modestly
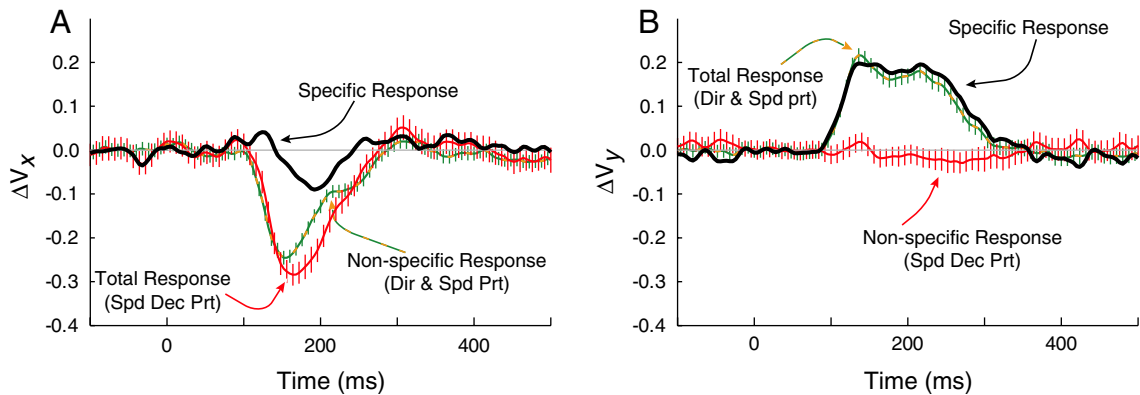
Fig. 13 The horizontal (**a**) and vertical (**b**) gaze velocity responses to perturbations. The traces depict averaged data from the *Speed Decrease* perturbations (in which the *x*-target velocity decreased transiently without a change in the *y*-velocity, *red lines*) and *Direction and Speed* perturbations (in which *y*-target velocity changed transiently but there was no change in the *x*-velocity, *green* and *yellow alternating lines*). Gaze velocities in each experimental condition were normalized with respect to target speed. The *thick black lines* represent the response specific to a perturbation in that direction. For the measured conditions (*Speed Decrease* and *Direction and Speed* perturbations) the ±95% confidence intervals are denoted with vertical hatching

(Fig. 5c). Furthermore, one would expect pursuit angular velocity to be proportional to image velocity in the perpendicular direction, and this expectation was satisfied (compare Figs. 2b, d with 7c). Thus, it appears that the image motion models can be modified for 2D motion.

Time course of pursuit angular velocity and speed

Qualitatively, the pursuit angular velocity response evoked by a step change in the target's angular velocity resembled changes in pursuit speed followed by a step change in target speed during linear target motion (Huebner et al. 1992; Krauzlis and Lisberger 1994b; Robinson et al. 1986). After a time delay of approximately 100 ms, pursuit angular velocity increased rapidly, overshooting the target angular velocity, with subsequent damped oscillations (see Fig. 2b, d). When target angular velocity dropped back to zero, pursuit angular velocity decayed to zero following an approximately exponential time course with an undershoot. The steady state angular velocity matched the target's angular velocity up to 400°pa/s (Fig. 4); thereafter, the response saturated (Mrotek 2005). For linear target motion, pursuit speed also shows a saturating response at speeds exceeding 80°/s (Lisberger et al. 1981; Meyer et al. 1985).

The initial overshoot in pursuit angular velocity could be substantial, ranging from about 15% at high target angular velocities to more than 275% at low angular velocities (Fig. 3). Similar nonlinear trends, but of smaller magnitude, have been described for the overshoot in pursuit speed following the onset of linear target motion (Krauzlis and Lisberger 1994b), and this overshoot has been attributed to the existence of a "motion transient" component in the feedback pathway (Krauzlis and Lisberger 1994a). This explanation could potentially account for the present results as well, if such transients are evoked whenever there is an abrupt change in target motion (i.e., in speed or angular velocity). However, it should be noted that image velocity in the direction perpendicular to the path also shows an initial overshoot (Fig. 7c), whose magnitude is comparable to the magnitude of the overshoot in angular velocity (Fig. 8a). Consequently, it is possible that feedback of image velocity, per se, is adequate to account for the time course of pursuit angular velocity without the need to invoke additional components.

During the curve, speed decreased slowly (Fig. 5c), by an amount that depended on the target's angular velocity (Fig. 6). This aspect of the behavior is also in accord qualitatively with image motion feedback models. The component of target velocity in the direction of smooth pursuit is proportional to $\cos(\delta\theta)$, where $\delta\theta$ is the angular difference between the direction of target motion and the direction of pursuit (Fig. 5a). To a first approximation, $\delta\theta$ is equal to $\tau\dot{\Theta}_T$ where $\dot{\Theta}_T$ is the target's angular velocity and τ is the directional lag (Fig. 5b). Since the target's angular velocity did not change during the curve, changes in gaze speed should be qualitatively related to the magnitude of the directional lag. By comparing Fig. 5b and c, one can see that when the directional lag increases, gaze speed decreases (e.g., 0–200 and 400–500 ms). This explains the initial decrease in speed (to approximately 750 ms), but does not account for the gradual increase in the latter half of the curve.

Anisotropies in pursuit gain

Thus, the time course of the modulations in pursuit speed and angular velocity could be accounted qualitatively by a negative feedback of image velocity. This was verified quantitatively (see Table 2). The components of

eye acceleration in directions parallel $(A_{\parallel g})$ and perpendicular $(A_{\perp g})$ to the direction of pursuit were strongly correlated with the corresponding components of image velocity $(V_{\perp \text{im}}, V_{\parallel \text{im}})$, provided they were shifted appropriately in time. On average, the correlation in the perpendicular direction was higher than the correlation in the parallel direction (coefficient of determination 0.85 compared to 0.64). This should not be surprising because the perpendicular image velocity was much larger than the parallel image velocity (Fig. 7c, d). Pursuit gain in the perpendicular direction (9.8 s^{-1}) on average was about twice as large as the gain in the parallel direction. Despite the uncertainty in estimating this latter gain, the difference in the gains was a consistent finding and it was unexpected. The results of the perturbation experiments also suggested that gain was higher in the perpendicular direction. The gain anisotropy cannot be easily attributed to the disparity in the image velocities in the two directions because gain has been shown to decrease as the amplitude of a target speed perturbation is increased (Churchland and Lisberger 2001, 2002).

Anisotropies in pursuit gain have been reported under a variety of experimental conditions. For example, pursuit gain for linear target motion is higher along the horizontal direction than it is along the vertical (Baloh et al. 1988; Collewijn and Tamminga 1984; Rottach et al. 1996), and it is reported to be smallest along oblique directions (Krukowski and Stone 2005). The response to small perturbations imposed during ongoing pursuit of linear target motion also shows directional anisotropies. Specifically, Schwartz and Lisberger (1994) found that the gain parallel to the direction of target motion was greater than the gain in the perpendicular direction, irrespective of whether the unperturbed motion was vertical or horizontal. This latter experiment provided a clear demonstration of a state-dependent gain control of smooth pursuit (see also Carey and Lisberger 2004).

Our results also suggest a state-dependent modulation of pursuit gain, but they differ from those of Schwartz and Lisberger (1994) in a fundamental manner. Our analysis suggests that pursuit gain was highest in the direction perpendicular to gaze velocity, whereas they found that it was highest in the tangential direction. We believe the discrepancy arises from the nature of the retinal image errors that can be expected to occur for quasipredictable target motions. For linearly moving targets, such errors can be expected to be largest in the direction of motion. For a circularly moving target, errors in the direction perpendicular to the target's motion can be expected to be largest, because the direction of pursuit always lags the target's motion (Fig. 5a).

The results of brief directional perturbations applied at the onset of circular target motion support this interpretation. When the target consistently curved upwards on every trial, there was a clear difference in the response to upwardly and downwardly directed pertur-

bations, the response for upward perturbations being larger (Fig. 10d). By contrast, when there was an equal probability of circular motion in the clockwise and counterclockwise direction, this asymmetry in the responses was no longer present (Fig. 10f).

Our analysis suggests that the directional anisotropy in pursuit gain varies with time when it is expressed in space-fixed coordinates (i.e., with respect to vertical or horizontal). In our analysis, we computed gain over the entire duration of the circular target motion. The gain in the perpendicular direction was nearly twice the gain in the parallel direction, but in both cases, the gain was relatively constant as the perpendicular direction changed from vertical (before the curve) to horizontal (during the curve). (Note that our analysis does not preclude the possibility that the directional modulation of the gain led or lagged the direction of pursuit.)

We also attempted to directly probe pursuit gain at the onset of circular target motion by applying brief perturbations to the target's motion in different directions. The perturbations elicited a transient decrease in speed, irrespective of the direction of the perturbation (Fig. 11). We previously found such a nonspecific decrement in speed when the target changed direction abruptly (Soechting et al. 2005). We did attempt to estimate the gain in the tangential direction by assuming a linear summation of a nonspecific response (i.e., a motion transient, Krauzlis and Lisberger 1994a) and one graded with the perturbation (Fig. 13). Under this assumption, the gain in the parallel (x) direction is smaller than the gain in the perpendicular (y) direction (Fig. 13).

In summary, our results are consistent with the notion that pursuit of targets moving in two dimensions is governed by image motion feedback and that the gain of this feedback is under online control. More specifically, our results suggest that this gain control is based on expectations about the target's trajectory and in particular, the nature of the retinal errors encountered during its pursuit.

References

Bahill AT, McDonald JD (1983) Smooth pursuit eye movements in response to predictable target motions. Vis Res 23:1573–1583

Baloh RW, Yee RD, Honrubia V, Jacobson K (1988) A comparison of the dynamics of horizontal and vertical smooth pursuit in normal human subjects. Aviat Space Environ Med 59:121–124

Barnes GR (1982) A procedure for the analysis of nystagmus and other eye movements. Aviat Space Environ Med 53:676–682

Barnes GR, Barnes DM, Chakraborti SR (2000) Ocular pursuit responses to repeated, single-cycle sinusoids reveal behavior compatible with predictive pursuit. J Neurophysiol 84:2340–2355

Bennett SJ, Barnes GR (2003) Human ocular pursuit during the transient disappearance of a visual target. J Neurophysiol 90:2504–2520

Bennett SJ, Barnes GR (2004) Predictive smooth ocular pursuit during the transient disappearance of a visual target. J Neurophysiol 92:578–590

van den Berg AV (1988) Human smooth pursuit during transient perturbations of predictable and unpredictable target movement. Exp Brain Res 72:95–108

Carey MR, Lisberger SG (2004) Signals that modulate gain control for smooth pursuit eye movements in monkeys. J Neurophysiol 91:623–631

Churchland MM, Lisberger SG (2001) Experimental and computational analysis of monkey smooth pursuit eye movements. J Neurophysiol 86:741–759

Churchland AK, Lisberger SG (2002) Gain control in human smooth-pursuit eye movements. J Neurophysiol 87:2936–2945

Collewijn H, Tamminga EP (1984) Human smooth and saccadic eye movements during voluntary pursuit of different target motions on different backgrounds. J Physiol (Lond) 351:217–250

Dallos PJ, Melvill-Jones RW (1963) Learning behavior of the eye fixation control system. IEEE Trans Autom Contr AC 8:218–227

Deno DC, Crandall WF, Sherman K, Keller EL (1995) Characterization of prediction in the primate visual smooth pursuit system. Biosystems 34:107–128

de'Sperati C, Viviani P (1997) The relationship between curvature and velocity in two-dimensional smooth pursuit eye movements. J Neurosci 17:3932–3945

Engel KC, Soechting JF (2003) Interactions between ocular motor and manual responses during two-dimensional tracking. Progr Brain Res 142:141–153

Engel KC, Anderson JH, Soechting JF (1999) Oculomotor tracking in two dimensions. J Neurophysiol 81:1597–1602

Engel KC, Anderson JH, Soechting JF (2000) Similarity in the response of smooth pursuit and manual tracking to a change in the direction of target motion. J Neurophysiol 84:1149–1156

Fender DH (1971) Time delays in the human eye tracking system. In: Bach-y-Rita P, Collins CC, Hyde JE (eds) The control of eye movements. Academic, New York

Huebner WP, Leigh RJ, Seidman SH, Thomas CW, Billian C, DiScenna AO, Dell'Osso LF (1992) Experimental tests of a superposition hypothesis to explain the relationship between the vestibuloocular reflex and smooth pursuit during horizontal combined eye–head tracking in humans. J Neurophysiol 68:1775–1792

Keller EL, Heinen SJ (1991) Generation of smooth-pursuit eye movements: neuronal mechanisms and pathways. Neurosci Res 11:79–107

Kettner RE, Leung HC, Peterson BW (1996) Predictive smooth pursuit of complex two-dimensional trajectories in monkey: component interactions. Exp Brain Res 108:221–235

Kowler E (1989) Cognitive expectations, not habits, control anticipatory smooth oculomotor pursuit. Vis Res 29:1049–1057

Kowler E, Steinman RM (1981) The effect of expectations on slow oculomotor control-III. Guessing unpredictable target displacements. Vis Res 21:191–203

Kowler E, Martins AJ, Pavel M (1984) The effect of expectations on slow oculomotor control-IV. Anticipatory smooth eye movements depend on prior target motions. Vis Res 24:197–210

Krauzlis RJ (2004) Recasting the smooth pursuit eye movement system. J Neurophysiol 91:591–603

Krauzlis RJ, Lisberger SG (1989) A control systems model of smooth pursuit eye movements with realistic emergent properties. Neur Comput 1:116–122

Krauzlis RJ, Lisberger SG (1994a) A model of visually-guided smooth pursuit eye movements based on behavioral observations. J Comput Neurosci 1:265–283

Krauzlis RJ, Lisberger SG (1994b) Temporal properties of visual motion signals for the initiation of smooth pursuit eye movements in monkeys. J Neurophysiol 72:150–162

Krukowski AE, Stone LS (2005) Expansion of direction space around the cardinal axes revealed by smooth pursuit eye movements. Neuron 45:315–323

Leung HC, Kettner RE (1997) Predictive smooth pursuit of complex two-dimensional trajectories demonstrated by perturbation responses in monkeys. Vis Res 37:1347–1354

Lisberger SG, Evinger C, Johanson GW, Fuchs AF (1981) Relationship between eye acceleration and retinal image velocity during foveal smooth pursuit in man and monkey. J Neurophysiol 46:229–249

Lisberger SG, Morris EJ, Tychsen L (1987) Visual motion processing and sensory-motor integration for smooth pursuit eye movements. Annu Rev Neurosci 10:97–129

Meyer CH, Lasker AG, Robinson DA (1985) The upper limit of human smooth pursuit velocity. Vis Res 25:561–563

Mrotek L (2005) Influence of direction during target tracking. PhD Thesis, University of Minnesota, p 274

Mrotek LA, Flanders M, Soechting JF (2004) Interception of targets using brief directional cues. Exp Brain Res 156:94–103

Robinson DA, Gordon JL, Gordon SE (1986) A model of the smooth pursuit eye movement system. Biol Cybern 55:43–57

Roitman AV, Massaquoi SG, Takahashi K, Ebner TJ (2004) Kinematic analysis of manual tracking in monkeys: characterization of movement intermittencies during a circular tracking task. J Neurophysiol 91:901–911

Rottach KG, Zivotofsky AZ, Das VE, Averbuch-Heller L, Discenna AO, Poonyathalang A, Leigh RJ (1996) Comparison of horizontal, vertical and diagonal smooth pursuit eye movements in normal human subjects. Vis Res 36:2189–2195

Schwartz JD, Lisberger SG (1994) Initial tracking conditions modulate the gain of visuo-motor transmission for smooth pursuit eye movements in monkeys. Vis Neurosci 11:411–424

Soechting JF, Mrotek LA, Flanders M (2005) Smooth pursuit tracking of an abrupt change in target direction: vector superposition of discrete responses. Exp Brain Res 160:245–258